

Categorization of various methods for quantitative susceptibility mapping (QSM) and their noise properties

Shuai Wang¹, Tian Liu², Weiwei Chen³, Cynthia Wisnieff², Pascal Spincemaille², A.John Tsiouris², and Yi Wang²

¹School of Electronic and Engineering, University of Electronic Science and Technology of China, Chengdu, Sichuan, China, ²Department of Radiology, Weill Cornell Medical College, New York, New York, United States, ³Department of Radiology, Tongji Hospital, Tongji Medical College, Huazhong University of Science & Technology, Wuhan, Hubei, China

TARGET AUDIENCE: anyone interested in tissue magnetic property

INTRODUCTION: Quantitative susceptibility Mapping (QSM) has generated a lot of scientific interests^{1,2}. Many clinically acceptable single orientation QSM methods have been proposed to solve the ill-posed problem to obtain the susceptibility map³⁻¹⁰. To help understand these methods for future QSM standardization, we propose a systematic categorization and noise error analysis for various QSM methods.

THEORY: The forward problem is that the tissue local magnetic field is the convolution of the dipole kernel with the susceptibility distribution in image \mathbf{r} -space $\delta_b = d \otimes \chi + n$ [Eq.1], ($\delta_b = \delta_b(\mathbf{r})$ is the local field relative to main field B_0 , $d(\mathbf{r})$ the dipole kernel, $\chi(\mathbf{r})$ susceptibility distribution, $n(\mathbf{r})$ noise) or multiplication in \mathbf{k} -space as $\Delta_b = DX + N$ [Eq.2] ($\Delta_b(\mathbf{k}) = F\delta_b$, F is Fourier transform, $D(\mathbf{k}) = Fd$, $X(\mathbf{k}) = F\chi$, $N(\mathbf{k}) = Fn$). We propose to categorize various inverse solutions for QSM into the following four categories: **I) Non-Bayesian approach with alteration of the dipole kernel to overcome ill condition.** An example is the truncated \mathbf{k} -space method (TKD)⁶. **II) Non-Bayesian approach with approximation of the dipole kernel to overcome ill condition.** An example is weighted \mathbf{k} -space derivative (WKD)⁴ using L'Hospital's rule interpolation around the cone surface in \mathbf{k} -space. **III) Bayesian approach using a general mathematical prior:** $\chi = \text{argmin}\{E + \alpha M\}$ [Eq.3] (E is the data fidelity term specifying the likelihood and M a general mathematical regularization term). Examples of M include the gradient L_2 ⁸, gradient L_1 ^{8,9}, total variation norm, wavelet L_1 ⁵ and combination of two L_1 ⁵. **IV) Bayesian approach using specific physical structure prior:** $\chi = \text{argmin}\{E + \alpha P\}$ [Eq.4] (P is a prior specific to a physical situation). Examples of P is a structural consistency between magnitude and susceptibility $P = \|mG\chi\|_1$ [Eq.5]^{3,10}.

Noise is the major cause of error for the QSM inverse solutions. The noise in the magnetic field data has a complex distribution and only when $\text{SNR} \gg 1$ can be approximated as Gaussian to render a simple weighting factor ($w^2 = \text{SNR}(\mathbf{r})^2$, referred to as noise whitening) for noise effects in the field based data fidelity expression (linear w.r.t. field). In general, the data fidelity can be formulated (nonlinearly w.r.t. field) using complex MR data with Gaussian noise in real and imaginary parts¹⁰.

METHODS: TKD, WKD, TVWA (Eq.3, $E = \|z\|_2^2$, $z = d \otimes \chi - \delta_b$ and $\alpha M = \alpha \|\Phi\chi\|_1 + \beta \text{TV}(\chi)$ [Eq.6]⁵) and MGL1 (Eq.3, $E = \|z\|_2^2$ and Eq.5) were selected as the representatives of category I, II, III and IV respectively. Linear noise whitening was illustrated with LTVWA (Eq.3, $E = \|wz\|_2^2$, and Eq.6) and MEDI (Eq.3, $E = \|wz\|_2^2$ and Eq.5) from category III and IV, and nonlinear noise whitening was illustrated with NTVWA (Eq.3, $E = \|wz_n\|_2^2$ and Eq.5). Exhaustive parameter search for optimal recon was used for all QSMs. **1) A Zubal numerical phantom** with an additional lesion was constructed with known susceptibility. The Gaussian noise and the noiseless field perturbation are both simulated in complex and use Eq.2 at $B_0 = 3\text{T}$ and $\text{TE} = 20\text{ms}$. The lesion magnitude, noise level and background were set to the average value of five *in-vivo* images of same imaging parameters. **2) Consecutive patients (n=50)** (with IRB approval) were used to evaluate the noise whitening effects in category III & IV. Multi Echo 3D gradient data were acquired with $\text{TE}_1/\Delta\text{TE}/\text{TR} = 5.7/6.7/57\text{ms}$, # of $\text{TE} = 8$; 20° flip, 41.67Hz bandwidth, 24cm FOV, and resolution = $0.57 \times 0.75 \times 2 - 0.7 \times 0.7 \times 0.7\text{mm}^3$. A neuroradiologist (10 yrs' experience) reviewed all images blinded to reconstruction methods. Image quality was scored (1=corrupted by artifacts; 2=extensive artifacts; 3=substantial artifacts interfering perception; 4=minor artifacts not interfering perception; 5=free of artifacts). Wilcoxon test was used to assess statistical significance.

RESULTS: There were substantial streaking artifacts in all recon from noisy data compared to noiseless data (Figs.1a vs 1b). The root mean square error (RMSE) in lesion relative to true susceptibility was 156.50%, 154.40%, 135.56%, 10.24%, 9.82%, 110.82%, 2.19%, 2.06% for TKD, WKD, TVWA, LTVWA, NTVWA, MGL1, MEDI and NMEDI respectively. Fig.2 showed example patient images without (Fig.2a) and with (Fig.2b) hemorrhage. The overall QSM image scores for TVWA, LTVWA, NTVWA, MGL1, MEDI and NMEDI were 2.24 ± 0.62 , 2.82 ± 0.63 , 3.54 ± 0.64 , 3.34 ± 0.85 , 3.74 ± 0.78 and 4.02 ± 0.65 respectively. The overall image qualities were statistical different between no and linear/nonlinear noise whitening ($p < 0.02$).

DISCUSSION AND CONCLUSION: The noise causes severe artifacts in QSM inverse solution. Bayesian approach allows noise whitening to reduce artifacts. Data fidelity based on Gaussian approximation of noise in estimated field forms the linear noise whitening method, which can be improved by data fidelity based on true Gaussian noise in the complex MR signal, the nonlinear noise whitening method.

For Bayesian approach, the general mathematical prior may be improved with a prior specific to the imaging physical situation. For the illustrated QSM method, NMEDI using the Bayesian approach with a physical structural consistency prior provides the best QSM image quality.

REFERENCES: 1.Liu T, et al, MRM 2009;61:196. 2.Schweser F, et al, Neuroimage 2011;54:2789-2807. 3.Liu J, et al, Neuroimage.2012.59:2560. 4.Li W, et al, Neuroimage 2011;55:1645. 5.Wu B, et al, MRM 2012;67:137. 6. Shmueli K, et al, MRM 2009;62:1510. 7. Salomir R, et al, ConceptMR 2003;19B:26. 8.Kressler B, et al, IEE TMI 2010;29:273. 9.De Rochefort L, et al, MRM 2010;63:194. 10.Liu T, et al, MRM 2012, doi: 10.1002/mrm.24272.

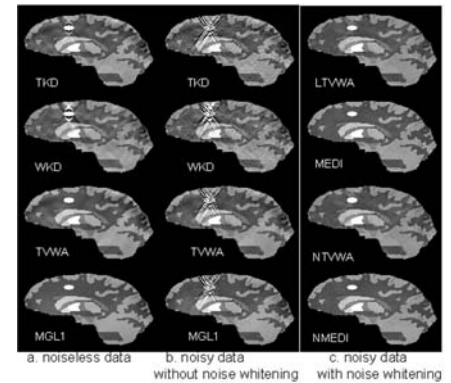


Fig 1. a) 4 QSM methods representing 4 categories. Noise artifacts (TVWA & MGL1 in b) are suppressed by linear noise whitening (LTVWA & MEDI in top c), and further suppressed by nonlinear noise whitening (NTVWA & NMEDI in bottom c).

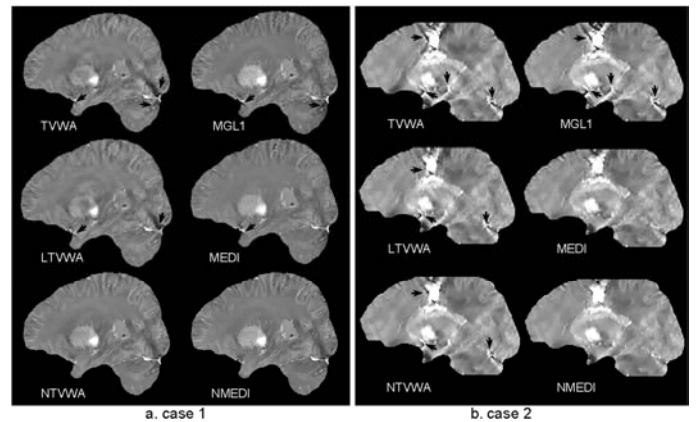


Fig 2. Noise whitening reduces artifacts (black arrows) in QSM of patients a) without and b) with hemorrhage. From top to bottom, scores of image quality (IQ) for TVWA/LTVWA/NTVWA = 3 / 4 / 5 in a) and 2 / 3 / 3 in b), IQ for MGL1/MEDI/NMEDI = 4 / 4 / 5 in a) and 3 / 4 / 4 in b).